THE JOURNAL OF PHYSICAL CHEMISTRY B LETTERS

2006, *110,* 24281−24286
Published on Web 10/31/2006

Microscopic Inhomogeneity and Ultrafast Orientational Motion in an Organic Photovoltaic Bulk Heterojunction Thin Film Studied with 2D IR Vibrational Spectroscopy

Larry W. Barbour, Maureen Hegadorn, and John B. Asbury*

Department of Chemistry, The Pennsylvania State University, University Park, Pennsylvania 16802

Received: August 30, 2006; In Final Form: September 25, 2006

Two-dimensional infrared vibrational spectroscopy is used to examine conformational inhomogeneity and ultrafast orientational motion within local environments of an organic photovoltaic bulk heterojunction thin film. The bulk heterojunction material consists of a mixture of the electron donor poly[2-methoxy-5-(2′-ethylhexyloxy)-1,4-(1-cyanovinylene)phenylene] (CN-MEH-PPV) and the electron acceptor [6,6]-phenyl-C_{61}-butyric acid methyl ester (PCBM). PCBM species reside in a distribution of environments within large domains of the molecules that cause their C═O stretch modes to be inhomogeneously broadened. The molecular inhomogeneity also results in frequency dependent vibrational relaxation dynamics. The butyric acid methyl ester group of PCBM undergoes ultrafast wobbling-in-the-cone orientational motion on the 110 fs time scale within a cone semiangle of 29°. The vibrational dynamics are sensitive metrics of molecular order in the material and have implications for charge mobility and degradation phenomena in organic photovoltaic devices. This report represents the first study of organic photovoltaic materials using ultrafast two-dimensional infrared vibrational spectroscopy.

I. Introduction

Organic photovoltaic (OPV) devices have been actively studied as alternatives to traditional inorganic photovoltaics because of their promise for economical solar power generation.[1,2] Current efforts to enable practical OPV devices focus on their efficiency and operational lifetime.[1,3−5] The efficiency is largely limited by low carrier mobility in the photovoltaic active layer, which consists of a bulk heterojunction of electron donating and accepting materials.[4,5] The microstructure of the bulk heterojunction strongly influences the carrier mobility and thus the short-circuit current of photovoltaic devices.[6,7] The operational lifetime of OPV devices is limited by photochemical reactions that degrade the active layer.[3,8] A critical step in the advancement of OPV technology is the elucidation of molecular factors that influence carrier mobility and degradation by direct examination of the chemical structures and their dynamics.

Recent advances in ultrafast two-dimensional infrared vibrational (2D IR) spectroscopy have provided a new approach to explore the structure and dynamics of condensed phase systems through molecular vibrations. In particular, 2D IR spectroscopy has been utilized to study ultrafast hydrogen bond network dynamics in water[9,10] and other systems.[11−14] 2D IR spectroscopy has also been used to examine vibrational coupling in model DNA helices,[15] vibrational dynamics of membrane proteins,[16,17] and secondary structures in proteins.[18−21]

Here we report the first study of an OPV bulk heterojunction thin film using ultrafast 2D IR spectroscopy. The 2D IR method is sensitive to the molecular order in bulk heterojunction materials by probing their native vibrational modes. The technique also enables direct examination of chemical transformations associated with degradation in the materials, although this topic will be addressed in a separate publication.[22] The components of the bulk heterojunction examined in this study are displayed in structure I and consist of a mixture of poly-

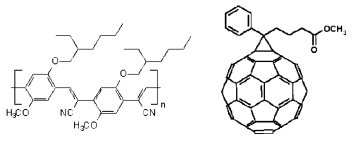

CN-MEH-PPV **PCBM**

[2-methoxy-5-(2′-ethylhexyloxy)-1,4-(1-cyanovinylene)phenylene] (CN-MEH-PPV) as the electron donor and [6,6]-phenyl-C_{61}-butyric acid methyl ester (PCBM) as the electron acceptor. In this contribution, we focus on the C═O stretch of PCBM, which appears at 1740 cm^{-1}.

II. Experimental Methods

A detailed description of the experimental methods will be provided elsewhere.[23] Briefly, an ultrafast Ti:sapphire laser (Quantronix, Integra-CE) is used to pump an optical parametric amplifier (Light Conversion). Mid-infrared pulses at 5.8 μm are produced at 1 kHz with 6 μJ/pulse and 150 fs duration by difference frequency generation in a $AgGaS_2$ crystal. The mid-infrared pulses are split into two beams for the pump and probe pulses with a 30:1 intensity ratio. Phase resolved 2D IR experiments are conducted in the frequency domain.[24,25] The pump beam is passed through a Fabry−Perot interferometer to create a continuously adjustable pump spectrum with a full width at half-maximum of ∼5 cm^{-1} and stabilized to within ±1 cm^{-1}. A 64 element dual mercury cadmium telluride array detector is used to capture 32 frequencies simultaneously through a spectrograph while facilitating single shot normalization. The

10.1021/jp065639p CCC: $33.50

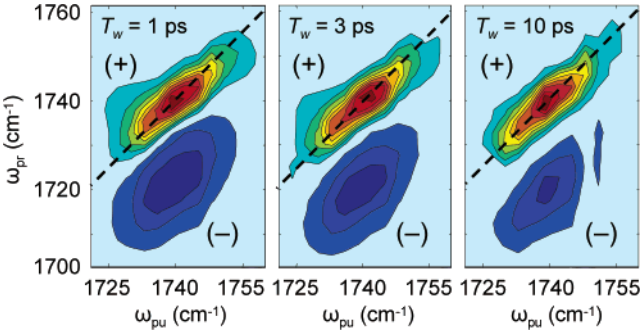

Figure 1. 2D IR spectra of the C═O stretch of PCBM in the bulk heterojunction at T_w delays of 1, 3, and 10 ps. The diagonals of the two-dimensional spectra are indicated with the dashed lines. The 0−1 transition is positive going and lies on the diagonal. The 1−2 transition is negative and is shifted off diagonal by the vibrational anharmonicity. Diagonal elongation of the 0−1 transition that persists to 10 ps indicates that spectral diffusion occurs very slowly.

entire infrared beam path and sample area are encompassed by a nitrogen purged enclosure to remove ambient H_2O and CO_2. The OPV mixture is prepared by combining PCBM (American Dye Source) and CN-MEH-PPV (H. W. Sands) in chlorobenzene (1.2% and 1.1%, respectively, by mass). The solution is drop cast onto a silver mirror and spun at 80 rpm to ensure the film dries uniformly. The silver mirror reflects the IR beams so that they do not encounter window materials in their overlap region and facilitates the examination of operational OPV cells that require one metallic electrode. All experiments are conducted at room temperature.

III. Results

The 2D IR spectra of the C═O stretch of PCBM in the OPV bulk heterojunction are displayed in Figure 1 at T_w delays of 1, 3, and 10 ps, where the T_w delay refers to the time separation between the pump and probe pulses. The two-dimensional spectra contain two frequency axes. The vertical axis, ω_{pr}, results from dispersing the probe beam into the spectrograph. The horizontal axis, ω_{pu}, corresponds to the frequency of the pump pulse at which a spectrum was recorded with the probe pulse. For the data displayed in Figure 1, a 3 cm^{-1} step between pump frequencies was used. The diagonals of the 2D IR spectra, where $\omega_{pr} = \omega_{pu}$, are represented by the dashed lines. The 2D IR spectra are plotted as change in transmission, where the contours represent 10% intervals of the maximum positive signal in each spectrum.

In 2D IR spectroscopy, the ground to first excited state (0−1) and the 1−2 transitions are accessed. The 0−1 transitions appear on the diagonals in Figure 1 and possess a positive sign because they correspond to the ground-state bleach and excited-state stimulated emission of the C═O stretch. The 1−2 transitions appear shifted off-diagonal along the ω_{pr} axis by the vibrational anharmonicity of 18 cm^{-1} and have a negative sign because they result from the excited-state absorption. The anharmonicity observed here is comparable to the value measured for the C═O stretch of methyl acetate in carbon tetrachloride.[26] The 0−1 and 1−2 transitions exhibit different line shapes in the 2D IR spectra. Similar behavior has been observed for the amide I band (C═O stretch) of *n*-methylacetamide where the behavior was explained in terms of the anharmonic vibrational potential of the C═O stretch mode.[27]

The 2D IR spectra displayed in Figure 1 are two-dimensional frequency maps correlating the frequency of a C═O stretch that was excited by the pump to its frequency when it interacted with the probe. Diagonal elongation of the 0−1 transition in the $T_w = 1$ ps spectrum indicates that C═O oscillators that were excited in a particular region of the transition do not exchange with oscillators from other regions on the few picosecond time scale, a process known as spectral diffusion.[9,28] In protein environments, the frequency of the C═O stretch of the polypeptide backbone, known as the amide I band, is sensitive to the structure of its local environment.[15,21,29−31] PCBM molecules in the bulk heterojunction exhibit a similar sensitivity. Inspection of the 2D IR spectra at $T_w = 3$ and 10 ps demonstrates that no significant spectral diffusion occurs within 10 ps (the 0−1 peaks retain the same shape), which indicates that local environments in the material exchange on a much longer time scale. Although the spectral shape is largely unchanged over the time period recorded in the 2D IR spectra, the amplitude of the signal decays by a factor of ∼100 due to vibrational relaxation. The corresponding decrease in the signal-to-noise ratio is exhibited by small distortions in 0−1 and 1−2 peak shapes in the 10 ps spectrum.

To gain additional information about the local environments surrounding PCBM molecules, vibrational relaxation and orientational diffusion dynamics of the C═O stretch were examined using ultrafast dispersed IR pump−probe spectroscopy. These experiments differ from the 2D IR experiments presented above in that the full laser spectrum is utilized in the pump pulse with a corresponding pulse duration of 150 fs. Pump−probe data collected with parallel pump and probe polarizations are displayed as change in transmission in Figure 2a. The horizontal axis, ω_{pr}, represents the probe frequency, and the vertical axis is the T_w delay time at which a probe spectrum was recorded. The time axis is plotted on a logarithmic scale to compress the time evolution at longer T_w delays for display purposes. The contours represent 7% intervals of the maximum positive signal.

Close inspection of the pump−probe data presented in Figure 2a demonstrates that the vibrational relaxation dynamics of the C═O stretch are frequency dependent. The dashed curves in Figure 2a indicate the frequencies where the maximum signal occurs for the 0−1 and 1−2 transitions as a function of the T_w delay. The shift is highlighted in Figure 2b where slices that were extracted at positions indicated by the dotted horizontal lines in Figure 2a are displayed together. In both cases the signal maxima shift to higher frequency with increasing time delay, indicating that the lower frequency portion of the C═O stretch has a shorter vibrational lifetime compared with the higher frequency region. We are able to eliminate spectral diffusion as a possible cause for the spectral shifts displayed in Figure 2 because the 2D IR spectra in Figure 1 indicate that this process does not occur on the 10 ps time scale.

The kinetics traces in Figure 3 display the time evolution of the pump−probe signal that is represented in Figure 2a at the probe frequency $\omega_{pr} = 1740$ cm^{-1} for parallel and also for perpendicular polarizations of the pump and probe pulses. Because spectral diffusion does not occur on the 10 ps time scale (see Figure 1), dynamics measured at a particular probe frequency reflect the evolution of a narrow distribution of C═O oscillators. Figure 3a depicts the data on a linear scale, and in Figure 3b the pure population relaxation trace, $P(T_w)$, is represented in a semilog plot. The pure population relaxation trace was calculated from the parallel, $S_{||}(T_w)$, and perpendicular, $S_{\perp}(T_w)$, traces using the relation

$$P(T_w) = (1/3)(S_{||}(T_w) + 2S_{\perp}(T_w)) \quad (1)$$

Overlaid on the population relaxation data and fit in Figure 3b is a dashed line that represents the appearance of an exponential

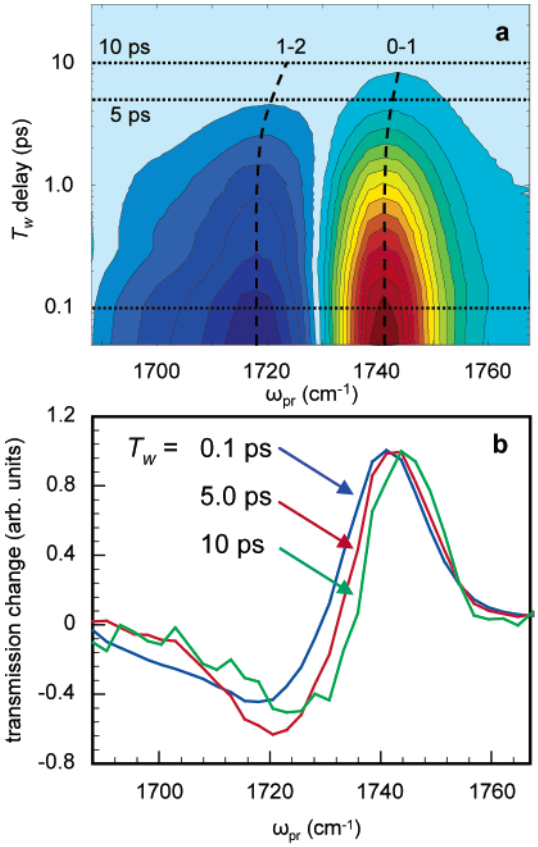

Figure 2. (a) Two-dimensional representation of ultrafast dispersed IR pump−probe spectra of the C═O stretch of PCBM in the bulk heterojunction material. The dashed lines represent the signal maxima for the 0−1 and 1−2 transitions as a function T_w delay. The dotted horizontal lines indicate the position on the time axis where one-dimensional frequency slices were extracted. (b) One-dimensional frequency slices highlighting the frequency dependent vibration lifetime of the C═O stretch of PCBM.

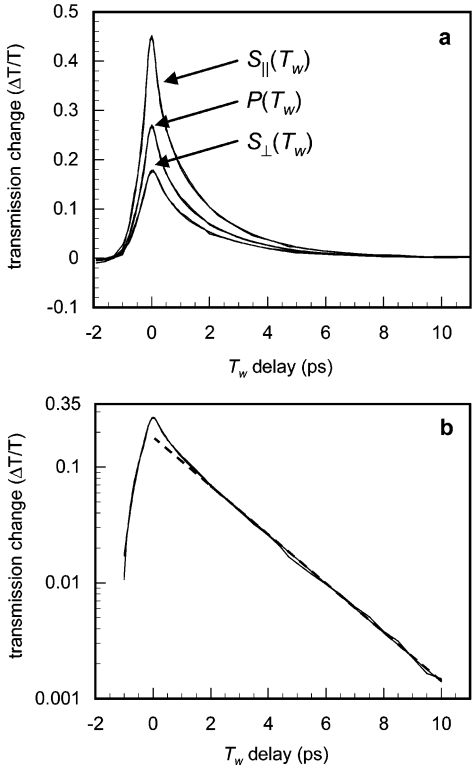

Figure 3. (a) Kinetics traces that show the time evolution of the IR pump−probe data displayed in Figure 2a. Traces collected with parallel and perpendicular polarizations between the pump and probe pulses are depicted from which the population relaxation kinetics trace was calculated. (b) Population relaxation kinetics trace plotted in a semilog plot. The dashed line represents the appearance of a single-exponential decay. The fit curves in both panels were calculated from models that are described in the text.

decay in a semilog plot. The comparison highlights the nonexponential vibrational relaxation dynamics of the C═O stretch primarily within the first 2 ps. The nonexponential behavior does not result from a nonresonant contribution. We use a reflective geometry where the pump and probe beams only overlap in the bulk heterojunction material that is deposited on a silver mirror. The beams do not encounter windows in their overlap region. We have determined that the nonresonant signal amplitude is negligible.

To quantify the nonexponential vibrational relaxation dynamics, the population relaxation trace in Figure 3 was fit with a model function, $F_P(T_w)$, described by the expression

$$F_P(T_w) = A[S_{FID}(T_w)\,\Theta(-T_w) + P(T_w)\,\Theta(T_w)] \otimes G(t) \quad (2)$$

where the arguments $P(T_w)$, $S_{FID}(T_w)$, and $G(t)$ have the following definitions:

$$P(T_w) = (1-b)\exp(-T_w/\tau_f) + b\exp(-T_w/\tau_s) \quad (3)$$

$$S_{FID}(T_w) = (1-a)\exp(-T_w^2/2\sigma_{FID}^2) + a\exp(-2|T_w|/\sigma_{FID}) \quad (4)$$

$$G(t) = (1/\sigma_{IR}\sqrt{2\pi})\exp(-t^2/2\sigma_{IR}^2) \quad (5)$$

and $\Theta(T_w)$ is the Heaviside step function. The model assumes a biexponential decay for the excited-state population dynamics, $P(T_w)$. Two time constants, τ_f and τ_s, describe the fast and slow decay components respectively. A mixed Gaussian and exponential description of the perturbed free induction decay of the C═O stretch, $S_{FID}(T_w)$, that appears at negative T_w delay is used where σ_{FID} represents the width parameter for both functions. The form of $S_{FID}(T_w)$ corresponds to the Fourier transform of a pseudo-Voigt function, which is needed to fit the linear IR spectrum. The symbol ⊗ represents a convolution of the bracketed expression with the instrument response, $G(t)$, that is characterized by a width parameter, σ_{IR}, corresponding to the convolution of the 150 fs IR pump and probe pulses. The best fit using eq 2 is displayed as a curve overlapping the population decay trace in Figure 3a,b. From the fit, we obtain time constants 0.40 and 2.0 ps, contributing 36% and 64% of the decay, respectively. The observed vibrational relaxation is remarkably similar to population dynamics recently measured by Tokmakoff and co-workers of the amide I band (C═O stretch) of *n*-methylacetamide.[27] To explain the nonexponential behavior, the authors considered vibrational coupling between the C═O bond and the C−N bond connected to it. A similar situation may exist in PCBM where the C═O bond may be coupled to its neighboring C−O single bond of the ester group. This vibrational coupling may introduce a fast relaxation channel out of the C═O excited-state that creates the nonexponential decay[27] observed in Figure 3.

Orientational relaxation dynamics can provide a sensitive probe of local environments in condensed phase systems.[32−34] Represented in Figure 4 is the anisotropy decay of PCBM molecules whose C═O stretch modes lie at the center of the transition at 1740 cm^{-1}. The anisotropy decay, $r(T_w)$, is related

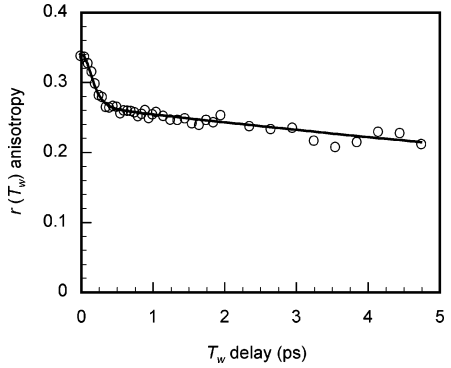

Figure 4. Orientational anisotropy decay of the C═O stretch of PCBM in the bulk heterojunction. The fit curve was calculated from a model that is described in the text.

to the orientational correlation function, $C_2(T_w)$, according to the expression

$$r(T_w) = 0.4C_2(T_w) = (S_{||}(T_w) - S_{\perp}(T_w))/(S_{||}(T_w) + 2S_{\perp}(T_w)) \quad (6)$$

where $S_{||}(T_w)$ and $S_{\perp}(T_w)$ are the parallel and perpendicular kinetics traces displayed in Figure 3a. We adopted the experimental methodology recently developed by Fayer and co-workers[35] to achieve the necessary control over signal amplitude for accurate anisotropy measurements. Because the nonresonant signal is negligible, we calculated the anisotropy decay starting from $T_w = 0$ ps. The shape and maximum value of the anisotropy decay [$r(0) = 0.34$] indicate that orientational motion of the C═O bond occurs on multiple time scales with a fast component that is similar to the pulse duration. Competition between excitation and orientational relaxation reduces the observed maximum anisotropy from the ideal value of 0.4 that would be measured if no fast orientational motion occurred. This fast orientational motion does not create an isotropic distribution. Instead, the anisotropy decays into a slow diffusive component that does not relax within the vibrational lifetime of the C═O stretch.

The behavior represented in Figure 4 is characteristic of wobbling-in-the-cone motion.[36,37] To quantify the orientational motion, we fit the anisotropy decay with the function

$$F_r(T_w) = 0.4C_2(T_w) \otimes G(t) \quad (7)$$

in which the form of the orientational correlation function, $C_2(T_w)$, is[33,38]

$$C_2(T_w) = (Q^2 + (1 - Q^2)\exp(-T_w/\tau_c))\exp(-T_w/\tau_m) \quad (8)$$

Equation 7 represents the convolution of the orientational correlation function with the instrument response function, $G(t)$ (see eq 5). Q^2 is the generalized order parameter that characterizes the cone semiangle in which fast orientational motion occurs. The time constants τ_c and τ_m are the time scales for orientational motion in the cone and slower diffusive motion, respectively. The best fit of the anisotropy decay using eq 7 is represented as the solid line in Figure 4. From the fit, fast orientational motion occurs with a time constant of $\tau_c = 110$ fs, and slower diffusive orientational motion occurs on the $\tau_m = 22$ ps time scale. The order parameter Q^2 characterizes the wobbling-in-the-cone semiangle θ according to the relation

$$Q^2 = [1/2(\cos\theta)(1 + \cos\theta)]^2 \quad [33] \quad (9)$$

The value of Q^2 from the fit is 0.67, corresponding to a cone semiangle of $\theta = 29°$. The fitting parameters for the anisotropy decay and the vibrational relaxation were used to calculate curves for the parallel and perpendicular decay traces in Figure 3a using the expression

$$F_x(T_w) = A[(S_{FID}(T_w)\,\Theta(-T_w) + P(T_w)\,\Theta(T_w))(1 + xC_2(T_w))] \otimes G(t) \quad (10)$$

which is a combination of eqs 2 and 7. The parameter x has the values +0.8 and −0.4 for the parallel and perpendicular kinetics traces, respectively.[39] The fidelity of the agreement between the calculated curves that are overlaid on the data in Figure 3a confirms that the data are consistent with the reported anisotropy decay.

IV. Discussion

Below, the experimental results and data analysis presented in the preceding section are synthesized to gain insight into local molecular environments found in the bulk heterojunction material. The inhomogeneity of the C═O stretch that is evidenced in the 2D IR data (see Figure 1) indicates that PCBM molecules sample a distribution of environments. The variety of environments creates frequency dependent vibrational relaxation dynamics (see Figure 2). We interpret the molecular origin of the inhomogeneity in the C═O stretch according to two observations that are described below. In a separate ultrafast visible pump-IR probe investigation (to be presented subsequently), we observed that PCBM molecules residing on the high-frequency side of the C═O stretch transition are preferentially involved in electron transfer with CN-MEH-PPV.[22] This observation can be interpreted in terms of the morphological framework recently reported by Sariciftci and co-workers who found that PCBM molecules aggregate into domains of ∼100 nm diameter when spin-cast with MDMO−PPV from chlorobenzene.[6,7] The MDMO−PPV formed a thin "skin" around the domains of PCBM. Given that the exciton diffusion length in organic materials is ∼10 nm,[4,5] only PCBM molecules residing in the outer shell of the domains can participate in electron transfer with the polymer.

Correlating this morphology with our ultrafast visible pump-IR probe experiments[22] suggests that PCBM molecules in the outer shell of the domains have higher frequency C═O stretches whereas molecules in the core of the domains reside on the lower frequency side of the transition. From these observations, we assign the inhomogeneous broadening displayed in Figure 1 to a distribution of shell versus core environments of PCBM molecules in the bulk heterojunction material. The microscopic origin of this frequency dependence on position within a PCBM domain has yet to be determined but may be related to the local electric field in the domain. This interpretation assumes that the PCBM domains in our film are much larger than the exciton diffusion length. We are in the process of determining this directly. For now we note that Sariciftci and co-workers demonstrated that large domains (>100 nm) of PCBM readily form,[6,7] so we are confident in the validity of our assumption.

From the analysis of the anisotropy data (see Figure 4), the butyric acid methyl ester group of PCBM experiences ultrafast restricted orientational motion on the 110 fs time scale within a cone semiangle of 29°. The inverse of the 110 fs time constant would correspond to ballistic motion of a 300 cm^{-1} mode. Based on a comparison of low-frequency vibrational modes of *n*-hexane, we expect the wobbling-in-the-cone motion to involve

a variety of stretching and bending modes in the 300−500 cm^{-1} region[40,41] that are probably not ballistic.

Following wobbling-in-the-cone orientational motion, PCBM molecules appear to undergo diffusive orientational motion on the 22 ps time scale. Ultrafast orientational dynamics have been observed for C_{60} in chlorobenzene[42,43] and in solid matrixes[44,45] near room temperature on the 10 ps time scale. This fast orientational motion results from the symmetry of C_{60} (essentially a sphere) and from its largely slip type intermolecular motion.[42,43] PCBM molecules can be considered a fullerene with a tether, and so it is not surprising that similar fast orientational motion is observed here. We do not anticipate that excitation transfer is a significant depolarization process in this system. The average distance between PCBM molecules residing in aggregates of pure PCBM is approximately 10 Å. The distance is greater for molecules dispersed between CN-MEH-PPV chains. This separation is large compared to similar studies where excitation transfer does not contribute significantly to depolarization.[33,38]

We eliminated alternate explanations of the biphasic orientational relaxation on the basis of the ultrafast time scale of the fast component. Alternate explanations include the possibility that inhomogeneous environments in the film produce a variety of orientational relaxation rates whose sum produces nonexponential behavior. Another model suggests that because PCBM does not possess spherical symmetry, reorientation about its nonequivalent axes of rotation results in the nonexponential dynamics. The fast orientational component observed here is ∼100 times faster than the time scale for reorientation that is observed for C_{60}. This disparity in time scales suggests that the fast component does not involve motion of the whole PCBM molecule, which points to the butyric acid methyl ester group. This reasoning in turn supports the wobbling-in-the-cone model because full depolarization most likely includes motion of the whole molecule. We should emphasize that the short vibrational lifetime of the C═O stretch prevents us from resolving the complete orientational dynamics of PCBM. Consequently, we are unable to comment on whether local environments or molecular asymmetry might produce nonexponential dynamics in the slow orientational component. The 22 ps time scale of the slow component is approximate for the same reason.

It is intriguing that PCBM molecules experience ultrafast orientational motion with apparently no corresponding spectral diffusion on the 10 ps time scale. The model of inhomogeneous broadening presented above is consistent with this observation. If the position within the C═O transition is determined by the residence of a PCBM molecule in the shell versus the core of a PCBM domain, then it is reasonable to anticipate that spectral diffusion would be extremely slow (much longer than 10 ps) because mass transport over the 10−100 nm length scale in solids is quite slow. In contrast, orientational diffusion does not necessarily involve mass transport within the domain, but rather rotation about the center of mass of the molecule. PCBM molecules can reorient without moving significantly in a domain, so this process is not associated with spectral diffusion on the 10 ps time scale.

On the basis of the results presented here, we speculate that the ultrafast infrared vibrational experiments reported here may provide an important probe into the microscopic environments of molecules in OPV materials. In addition to the inhomogeneous broadening of vibrational modes, the frequency dependence of vibrational lifetimes and cone semiangles over which vibrational modes can fluctuate are likely to be sensitive metrics of local topology. For example, a PCBM molecule residing at the interface between a PCBM domain and the polymer may exhibit a cone semiangle different from those of molecules in the core of a domain because of the different packing configurations available to the two materials. The model by which we interpret our results suggests that the cone semiangle should be frequency dependent for the same reason. We are in the process of exploring these and other topological/vibrational correlations that will be the focus of future publications.

V. Concluding Remarks

Ultrafast 2D IR vibrational spectroscopy was used to examine microscopic inhomogeneity and ultrafast orientational dynamics of the functionalized fullerene PCBM in an organic photovoltaic bulk heterojunction composed of a mixture of PCBM and the electron donor CN-MEH-PPV. This contribution represents the first application of 2D IR spectroscopy to the study of photovoltaic thin film materials. It was found that PCBM molecules reside in a distribution of environments within large domains of PCBM species in the bulk heterojunction with CN-MEH-PPV that cause their C═O stretch modes to be inhomogeneously broadened. Spectral diffusion within the C═O stretch occurred on time scales much longer than the vibrational lifetime, enabling vibrational relaxation dynamics of particular PCBM conformations to be accessed. The molecular inhomogeneity experienced by PCBM molecules results in a frequency dependent vibrational lifetime of the C═O stretch that depends on the detailed morphology of the local environment. The butyric acid methyl ester group of PCBM undergoes ultrafast wobbling-in-the-cone orientational motion on the 110 fs time scale within a cone semiangle of 29°. Inhomogeneity in the vibrational spectra, vibrational relaxation, and orientational dynamics are all expected to be sensitive metrics of local morphology having implications for carrier mobility and degradation phenomena in organic photovoltaic devices.

Acknowledgment. We thank the Camille and Henry Dreyfus New Faculty Awards Program and the Pennsylvania State University for support of this research.

References and Notes

(1) Brabec, C.; Sariciftci, N. S.; Hummelen, J. C. *Adv. Funct. Mater.* **2001**, *11*, 15.
(2) Brabec, C. J. *Sol. Energy Mater. Sol. Cells* **2004**, *83*, 273.
(3) Krebs, F. C.; Carle, J. E.; Cruys-Bagger, N.; Andersen, M.; Lilliedal, M. R.; Hammond, M. A.; Hvidt, S. *Sol. Energy Mater. Sol. Cells* **2005**, *86*, 499.
(4) Forrest, S. R. *Mater. Res. Soc. Bull.* **2005**, *30*, 28.
(5) Xue, J.; Rand, B. P.; Uchida, S.; Forrest, S. R. *Adv. Mater.* **2005**, *17*, 66.
(6) Hoppe, H.; Sariciftci, N. S. *J. Mater. Chem.* **2006**, *16*, 45.
(7) Hoppe, H.; Glatzel, T.; Niggemann, M.; Schwinger, W.; Schaeffler, F.; Hinsch, A.; Lux-Steiner, M. C.; Sariciftci, N. S. *Thin Solid Films* **2006**, *511*, 587.
(8) Halls, J. J. M.; Friend, R. H. Organic Photovoltaic Devices. In *Clean Energy from Photovoltaics*; Archer, M. D., Hill, R., Eds.; Imperial College Press: London, 2001; Vol. 1, pp 377.
(9) Asbury, J. B.; Steinel, T.; Stromberg, C.; Corcelli, S. A.; Lawrence, C. P.; Skinner, J. L.; Fayer, M. D. *J. Phys. Chem. A* **2004**, *108*, 1107.
(10) Eaves, J. D.; Loparo, J. J.; Fecko, C. J.; Roberts, S. T.; Tokmakoff, A.; Geissler, P. L. *Proc. Natl. Acad. Sci. U.S.A.* **2005**, *102*, 13019.
(11) Zheng, J.; Kwak, K.; Chen, X.; Asbury, J. B.; Fayer, M. D. *J. Am. Chem. Soc.* **2006**, *129*, 2977.
(12) Zheng, J.; Kwak, K.; Asbury, J. B.; Chen, X.; Piletic, I. R.; Fayer, M. D. *Science* **2005**, *309*, 1338.
(13) Huse, N.; Bruner, B. D.; Cowan, M. L.; Dreyer, J.; Nibbering, E. T. J.; Miller, R. J. D.; Elsaesser, T. *Phys. Rev. Lett.* **2005**, *95*, 147402.
(14) Kim, Y. S.; Hochstrasser, R. M. *Proc. Natl. Acad. Sci. U.S.A.* **2005**, *102*, 11185.
(15) Krummel, A. T.; Zanni, M. T. *J. Phys. Chem. B* **2006**, *110*, 13991.
(16) Mukherjee, P.; Kass, I.; Arkin, I. T.; Zanni, M. T. *Proc. Natl. Acad. Sci. U.S.A.* **2006**, *103*, 3528.

(17) Volkov, V.; Hamm, P. *Biophys. J.* **2004**, *87*, 4213.
(18) Smith, A. W.; Chung, H. S.; Ganim, Z.; Tokmakoff, A. *J. Phys. Chem. B* **2005**, *109*, 17025.
(19) Wang, J.; Chen, H.; Hochstrasser, R. M. *J. Phys. Chem. B* **2006**, *110*, 7545.
(20) Chung, H. S.; Khalil, M.; Smith, A. W.; Ganim, Z.; Tokmakoff, A. *Proc. Nat. Acad. Sci. U.S.A.* **2005**, *102*, 612.
(21) Woutersen, S.; Hamm, P. *J. Chem. Phys.* **2002**, *115*, 7737.
(22) Barbour, L. W.; Hegadorn, M.; Asbury, J. B., Manuscript in preparation.
(23) Manuscript in preparation.
(24) Hamm, P.; Lim, M.; DeGrado, W. F.; Hochstrasser, R. M. *J. Chem. Phys.* **2000**, *112*, 1907.
(25) Cervetto, V.; Helbing, J.; Bredenbeck, J.; Hamm, P. *J. Chem. Phys.* **2004**, *121*, 5935.
(26) Lim, M.; Hochstrasser, R. M. *J. Chem. Phys.* **2001**, *115*, 7629.
(27) DeFlores, L. P.; Ganim, Z.; Ackley, S. F.; Chung, H. S.; Tokmakoff, A. *J. Phys. Chem. B* **2006**, *110*, 18973.
(28) Tokmakoff, A.; Urdahl, R. S.; Zimdars, D.; Francis, R. S.; Kwok, A. S.; Fayer, M. D. *J. Chem. Phys.* **1995**, *102*, 3919.
(29) Mukherjee, P.; Krummel, A. T.; Fulmer, E. C.; Kass, I.; Arkin, I. T.; Zanni, M. T. *J. Chem. Phys.* **2004**, *120*, 10215.
(30) Bredenbeck, J.; Helbing, J.; Kumita, J. R.; Woolley, G. A.; Hamm, P. *Proc. Nat. Acad. Sci. U.S.A.* **2005**, *102*, 2379.
(31) Gnanakaran, S.; Hochstrasser, R. M.; Garcia, A. E. *Proc. Nat. Acad. Sci. U.S.A.* **2004**, *101*, 9229.
(32) Piletic, I. R.; Moilanen, D. E.; Spry, D. B.; Levinger, N. E.; Fayer, M. D. *J. Phys. Chem. A* **2006**, *110*, 4985.
(33) Tan, H.-S.; Piletic, I. R.; Fayer, M. D. *J. Chem. Phys.* **2005**, *122*, 174501.
(34) Rezus, Y. L. A.; Madsen, D.; Bakker, H. J. *J. Chem. Phys.* **2004**, *121*, 10599.
(35) Tan, H.-S.; Piletic, I. R.; Fayer, M. D. *J. Opt. Soc. Am. B* **2005**, *22*, 2009.
(36) Lipari, G.; Szabo, A. *Biophys. J.* **1980**, *30*, 489.
(37) Wang, C. C.; Pecora, R. *J. Chem. Phys.* **1980**, *72*, 5333.
(38) Gaffney, K. J.; Piletic, I. R.; Fayer, M. D. *J. Chem. Phys.* **2003**, *118*, 2270.
(39) Tokmakoff, A. *J. Chem. Phys.* **1996**, *105*, 1.
(40) Cates, D. A.; Strauss, H. L.; Snyder, R. G. *J. Phys. Chem.* **1994**, *98*, 4482.
(41) Mirkin, N. G.; Krimm, S. *J. Phys. Chem.* **1993**, *97*, 13887.
(42) Nichols, K. B.; Rodriguez, A. A. *J. Phys. Chem. A* **2005**, *109*, 3009.
(43) Martin, N. H.; Issa, M. H.; McIntyre, R. A.; Rodriguez, A. A. *J. Phys. Chem. A* **2000**, *104*, 11278.
(44) Johnson, R. D.; Yannoni, C. S.; Dorn, H. C.; Salem, J. R.; Bethune, D. S. *Science* **1992**, *255*, 1235.
(45) Hughes, E.; Jordan, J. L.; Gullion, T. *J. Phys. Chem. B* **2000**, *104*, 691.